ORIGINAL PAPER

METABOLOMIC ANALYSIS OF CHINESE YAM (*Dioscorea polystachya* Turczaninow) BULBILS AT DIFFERENT GERMINATION STAGES BY UPLC-Q-TOF-MS

Xiaojin Ge[1,2], Xiangyang Li[1], Dandan Dai[1], Zhen Yang[3], Yanhong Wang[1], Tiegang Yang[1], Guixiao La[1]

[1] Institute of Chinese Herbel Medicines, Henan Academy of Agricultural Sciences; Henan Provincial Center for Engineering and Technology Research of Traditional Chinese Medicine, Zhengzhou, Henan 450046, P.R. China

[2] School of Pharmaceutical Sciences, Guangzhou University of Chinese Medicine, Guangzhou, Guangdong 510006, P.R. China

[3] Xixian Agricultural Science Research Institute, Xinyang Henan 464300, P.R. China

ABSTRACT

Bulbil germination is crucial to the survival of Chinese yam plants, the preservation of germplasm resources and the worldwide supply of food and natural medicine. There are still some unknowns regarding bulbil biochemical variations associated with germination. The metabolic changes during the germination of Chinese yam (*Dioscorea polystachya* Turczaninow) bulbils were studied using ultrahigh-performance liquid chromatography coupled with quadrupole time-of-flight mass spectrometry (UPLC-Q-TOF-MS) at eight-time points covering all four phases of germination. It was determined that 27 metabolites, including organic acids, amino acids, sugars, lipid metabolites, phenolics and steroids, were responsible for the variation in the Chinese yam bulbil groups. A metabolomics pathway was proposed based on the identified metabolites. The main processes affected during germination were those related to carbohydrate metabolism, the TCA cycle, lipid metabolism, nitrogen metabolism, lipid metabolism and polyphenol metabolism. It is one of the earliest reports on the metabolite identification and profiling of Chinese yam bulbils at different germination stages.

Key words: Chinese yam bulbils, germination, metabolomics, UPLC-Q-TOF-MS, multivariate statistical analysis, metabolism pathway

INTRODUCTION

Chinese yam (*Dioscorea polystachya* Turczaninow) grows in temperate forests, scrub forests, herb communities, on mountain slopes, and along rivers and roadsides in China, Korea and Japan [Zhang 2014]. The species is widely cultivated in China, and its tubers are used as food and natural medicine [Padhan and Panda 2020]. Chinese yam is a monocotyledon genus and dioecious species. True seeds are produced when male and female plants grow in close proximity, but vegetative reproduction is far more common in the actual production of yam [Mizuki et al. 2010]. Bulbils and tuber heads are the most commonly used propagation organs [Kim et al. 2010]. Tuber heads are bulky to transport, and the multiplication rate in the field is very low [Dessalegn 2016]. Agronomic and quality characteristics will also decline with increasing planting years [Yu et al. 2021]. The bulbil propagation strategy, however, possesses the advantages of high reproductive efficiency and better retention of maternal genetic characteristics [Walck et al. 2010].

Chinese yam bulbils, similar to buds, are generated from axillary meristems at the axil, which are sometimes referred to as aerial tubers [Murty and Purnima 1983]. Bulbils have chemical compositions and nutrient substances similar to those of the tuber, such as essential amino acids, polysaccharides, flavonoids, phenolic acids and diosgenin [Choi et al. 2012, Narula et al. 2003]. It also provides a valuable food and medicinal ingredient source in people's everyday lives [Zhang et al. 2018]. The physiological structure of bulbils is distinct from that of seeds, but bulbils could be considered analogous to seeds from a dispersal viewpoint. Seeds and bulbils showed similar dormancy and germination characteristics [Okagami 1986].

At present, research on Chinese yam bulbils has mainly focused on their nutritional components [Zhang et al. 2018] and pharmacological effects [Chaniad et al. 2020]. Wu et al. [2019] performed a transcriptome study together with phytohormone analyses on critical developmental stages. They showed that auxin, CKs, ABA, and sucrose work together to provide forward signalling to transcription factors (from Aux/IAA, E2F, MYB, and bHLH families) that contribute to triggering bulbil formation and growth [Wu et al. 2019]. However, due to the complicated physiological metabolism and energy regulation of the germination process, the global metabolic response of energy-regulated germination of Chinese yam bulbils remains a mystery.

Metabolites represent the final product of gene expression, so they are usually considered the biochemical phenotype of an organism [Drummond and Renner 2022, Hill et al. 2014]. The use of metabolomics makes it easier to obtain comprehensive metabolic profiles during physiological processes in plants. Metabolomic analyses rely on research methods, such as gas chromatography–mass spectrometry, liquid chromatography–mass spectrometry, and nuclear magnetic resonance. Liquid chromatography–mass spectrometry, gas chromatography–mass spectrometry, and nuclear magnetic resonance were used to study the metabolic changes in brown rice [Kim H. et al. 2020], mung bean [Chen et al. 2019, Wu et al. 2020], soybean [Gu et al. 2017], and poplar seeds [Qu et al. 2019] during germination. Nevertheless, bulbils may have a different germination process than seeds due to their anatomical differences.

Currently, there is a lack of research on the metabolic mechanism of bulbil germination.

The objective of this work was to study the overall metabolic changes during the germination of Chinese yam bulbils using ultrahigh-performance liquid chromatography coupled with quadrupole time-of-flight mass spectrometry (UPLC-Q-TOF-MS). Differences in the samples were visualised by a principal component analysis (PCA) model and an orthogonal partial least squares discriminant analysis (OPLS-DA) model. Next, we identified the significant metabolites responsible for these differences and described a metabolomic pathway for energy production during germination.

MATERIALS AND METHODS

Materials. Chinese yam bulbils were collected in Jiaozhuo (China) in October 2022 and belonged to the same genotype. Analytical grade chemicals, including acetonitrile and formic acid (chromatographic purity), were purchased from Thermo Fisher Company (Waltham, MA, USA). NaClO was purchased from McLean Biochemical Technology Company Limited (Shanghai). Ultra-pure water was prepared using a Millipore Milli-Q purification system (Millipore Corp., Bedford, Mass., USA).

Germination treatment of Chinese yam bulbils. Three hundred Chinese yam bulbils with uniform size and plumps without pathological conditions were selected, each weighing approximately 1.5 g. All Chinese yam bulbils were sterilised in 3% (v/v) NaClO for 15 min and soaked in double distilled water for 12 h. After that, the soaked bulbils were placed in Petri dishes with sterilised absorbent cotton with double distilled water every 24 h and sprouted at 26°C in the dark with 75% relative humidity. Bulbils capable of germination were collected at 1, 2, 3, 5, 7, 10 and 15 days post imbibition. For each sample, nine biological replicates were independently analysed. All samples were snap-frozen in liquid nitrogen once collected and stored at –80°C until further analysis. Ungerminated soaked Chinese yam bulbils were used as a control (0 days).

Determination of moisture content, germination rate, and bud length. The moisture content of 80 Chinese yam bulbils during germination was determined using a moisture analyser (WL-70Y, Guanya, Shen-

zhen, China). The germination rate of 80 Chinese yam bulbils during germination was evaluated by visually counting the number. The bud length of the germinated bulbils was measured using a Vernier calliper (TWIN-CAL IP40, TESA, Renens, Switzerland) for 80 bulbils.

Sample preparation for UPLC-Q-TOF-MS analysis. Each frozen bulbil sample (300 mg) from the different germination stages was ground into fine powder in liquid nitrogen. Samples were then mixed with 1.5 mL prechilled solvent (85% aqueous methanol) and ultrasonically extracted for 30 min. Following centrifugation at 12,000 rpm for 10 min, the extracts were filtered through a 0.22 mm PTFE membrane filter before UPLC-Q-TOF-MS analysis.

Ultra-performance liquid chromatography-quadrupole-time-of-flight (UPLC-Q-TOF-MS) analysis. Metabolites extracted from Chinese yam bulbils by 85% aqueous methanol were analysed using an Acquity UPLC system (Waters, Milford, MA) connected to Xevo G2 Q-TOF MS equipped with an electrospray ionisation source (Waters, Milford, MA, USA). A gradient elution method was used for separating compounds by liquid chromatography. ACQUITY UPLC BEH C18 columns were used (2.1 mm by 100 mm by 1.7 m). The column temperature was maintained at 35°C, and the flow was set to 0.3 mL/min. The mobile phase consisted of solution A (water with 0.1% formic acid) and solution B (acetonitrile with 0.1% formic acid). From 1 to 18 minutes, elution was increased linearly from 5% B to 100% B. The injection volume was 5 μL. The eluted metabolites were analysed using the Q-TOF MS system with negative electrospray ionisation mode in the mass range of 50–2000 Da. The temperatures of the source and desolvation were set at 130°C and 350°C, respectively, and the desolvation flow rate was 700 L/h. Capillary, sampling and extraction cone voltages of 2.5 kV, 21 V and 4 eV, respectively, and a collision energy of 15 eV were used. Leucine-enkephalin ($[M – H] = 554.2615$) was used as a lock mass to ensure accuracy, which was detected during the run at a concentration of 500 pg/μL. All samples were mixed to prepare a quality control sample that was analysed before analysis began and after every ten analyses.

Data processing and multivariate statistical analysis. The mass chromatographic data acquisition and analyses of data were controlled by MassLynx v4.1 software (Waters Corp.), Progenesis QI v2.4 software (Waters Corporation, MA, USA) and UNIFI v1.8.2 software (Waters Corp.). All obtained chromatographic data were preprocessed and normalised to remove systematic as well as replicate variation within the samples. Then, the resultant data matrices were introduced into SIMCA-P v13.0.3 software (Umetrics, Umea, Sweden) for multivariate pattern recognition analysis, including principal component analysis (PCA) and orthogonal partial least squares discriminant analysis (OPLS-DA). The predictive parameters of the PCA model are R2X and Q2, while the predictive parameters of the OPLS-DA model are R2X, R2Y, and Q2. R2X and R2Y represent the interpretation rate of the model to the X and Y matrix, respectively, and Q2 indicates the prediction ability of the model. The closer these three indexes are to 1, the more stable and reliable the model is. Q2 > 0.5 can be regarded as an adequate model, and Q2 > 0.9 is an excellent model [Gao et al. 2020]. Based on the results of OPLS-DA, the metabolites with a VIP (variable importance in the project) value >0.8 were used to identify differential metabolites. VIP value (Variable Importance in Projection) is an indicator used to evaluate the correlation between a metabolite and sample classification. The higher the VIP value, the more significant the contribution of the metabolite to sample classification. Using SPSS 17.0 (SPSS Inc., Chicago, IL, USA), a one-way analysis of variance with Duncan's test (p-value < 0.05) was performed statistically on the discovered metabolites, moisture content, germination ratio, and bud length. Differences were considered to be statistically significant at p-value < 0.05.

RESULTS AND DISCUSSION

Germination-associated macroscopic phenotype changes for germinated Chinese yam bulbils. The morphologies of germinated Chinese yam bulbils are shown in Figure 1. Germination of bulbils begins with imbibition and ends with the appearance of distinct embryonic roots on the epidermis. According to the morphological changes in the bulbil germination process, it is mainly divided into four stages: dry (0 days), imbibition (1 day), emergence of shoots (2–5 days) and emergence of roots (7–10 days).

Fig. 1. Morphology of germinated Chinese yam bulbils according to the germination period
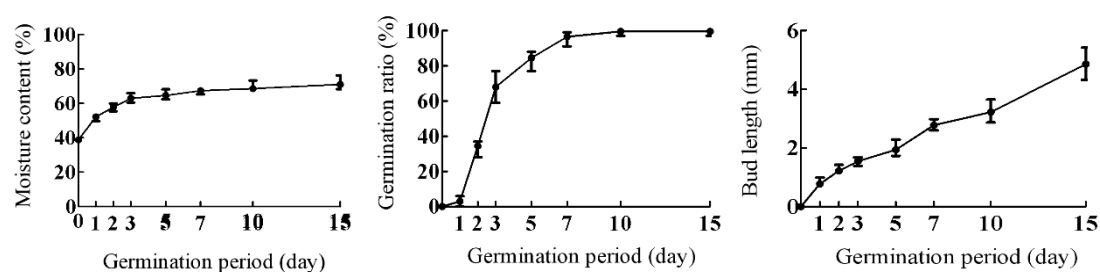
Fig. 2. Moisture content, germination ratio, and bud length of the Chinese yam bulbils according to the germination period. Moisture content increased from 38.8% to 71.0%, and germination ratio increased to 96.5% on day 7, bud length increased to 4.8 mm on day 15. Error bars are from 10 biological replicates

The general characteristics in terms of germination ratio, bud length, and moisture content are shown in Figure 2. The moisture content increased during germination by approximately 1.7 times on day 3 compared to day 0 (38.8%) and then gradually grew by 71.0% by 15 days. The germination ratio increased from 34.5% on day 2 to approximately 96.5% on day 7, and no further growth was observed after that. Bud length increased continuously, and the length on day 15 was approximately 4.8 mm.

Metabolomic analysis of germinated Chinese yam bulbils by UPLC-Q-TOF MS. The metabolite profiles of Chinese yam bulbils according to germination period (0, 1, 2, 3, 5, 7, 10 and 15 days) were characterised by UPLC-Q-TOF MS in negative ion mode. Figure 3 presents the based peak intensity chromatograms obtained from 0 days and 15 days of germinated Chinese yam bulbils.

After preprocessing with Progenesis QI software, which included the retention time (RT), m/z value, and normalised peak intensity, a data matrix was produced. A total of 1682 variables in the peak list were observed. SIMCA-P Software was used to perform multivariate statistical analysis on the peak list, which contained the retention time, m/z, and ion intensity of each sample. PCA was then used to analyse the peak list to distinguish between all samples from various germinated Chinese yam bulbils. Figure 2 displays the data plots of PCA scores. PCA was performed with UV scaling. $R2X = 0.751$ and $Q2 = 0.523$ indicated that the model made a reasonably good prediction. Based on the changes in their global chemical profiles, the PCA score plots (Fig. 4A) revealed that 72 samples of Chinese yam bulbils that had undergone germination could be divided into eight different clusters, each representing a different stage of germination. Notably, the groups were clearly divided between the non-germinated (0 days) and the germinated (15 days) groups. However, samples of 1, 2, 3, 5, 7, and 10 days of germinated Chinese yam bulbils were gathered

in their respective regions. It suggests that their metabolite variation may not be significant during these periods.

To obtain better discrimination among different germination stages of Chinese yam bulbils, the OPLS-DA approach was applied to enhance the separation among the groups in PCA. OPLS-DA was performed with Par scaling. As illustrated in the OPLS-DA score plot (Fig. 4B), the sample groups were clearly distinguished from one another with statistically acceptable quality parameters (R2X = 0.86 R2X = 0.829 Q2 = 0.581).

Identification of major metabolites. Prior to identifying the compounds, UNIFI v1.8.2 was used to add
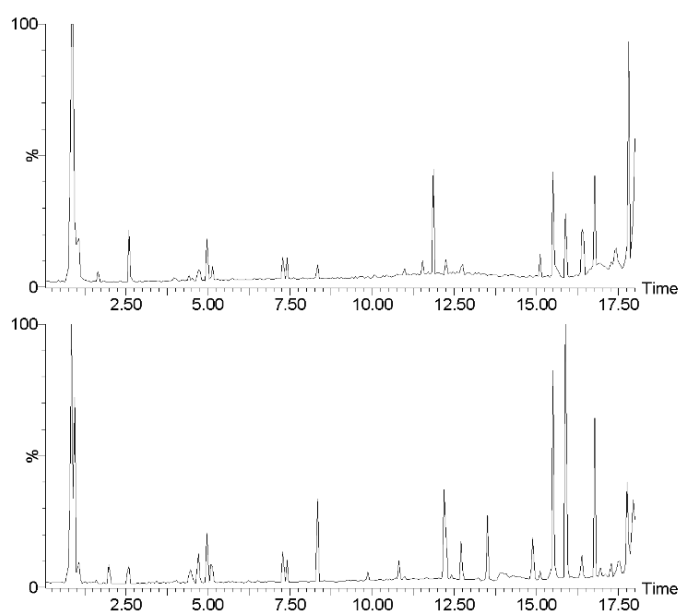
Fig. 3. Typical Based Peak Intensity chromatograms from UPLC-Q-TOF-MS of Chinese yam bulbils. The extracts of 0-day ungerminated bulbils (day 0) (A) and day 15 of germinated bulbils (B) were analysed in negative ion mode
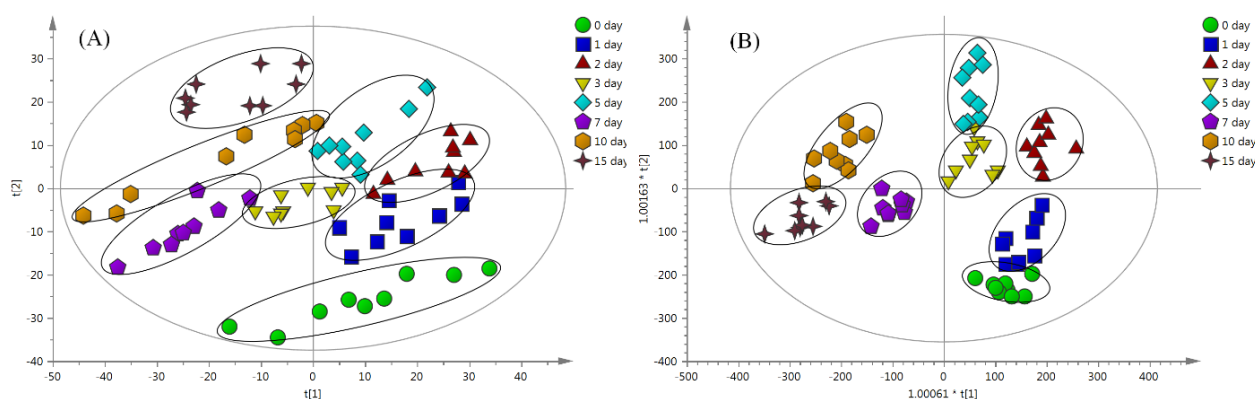
Fig. 4. The PCA score plot (A) and OPLS-DA score plot (B) show the germination-associated dynamic metabolomic phenotype changes for the Chinese yam bulbils

to an internal library that contained the compounds from Chinese yam based on the literature. Then, the m/z of ions from the raw data of Chinese yam was automatically matched to the library compounds. As a result, 27 metabolites, including amino acids (aspartic acid, glutamic acid, and tryptophan), organic acids (malic acid, citric acid, lactic acid, and p-coumaric acid), sugars (sucrose, raffinose, and glucose), lipid metabolites (linolenic acid, linoleic acid, palmitic acid, and oleic acid), steroid metabolites (protodioscin, desgalactotigonin, dioscin, and β-caucosterol), polyphenols (3,4',5-trihydroxy-3',7-dimethoxyflavone, apiin, 2,5-dihydroxy-3,4-dimethoxyphenanthrene, kaempferol-3-O-rutinoside, 3,3',5-trimethoxybibenzyl, batatasin I, and quercetin-3'-O-glucoside) and other metabolites (allantoin and hypoxanthine) (Tab. 1), were detected in the 85% aqueous methanol extract of Chinese yam bulbil. Based on the results of OPLS-DA and one-way analysis of variance, VIP and *p*-value of these metabolites were also recorded in Table 1. These metabolites with VIP > 0.8 and *p*-value < 0.05 were identified as the major contributors to the differences in the groups on the OPLS-DA score plot. Metabolites such as sugars, organic acids and lipids were also found during the germination of mung beans [Wu et al. 2020] and potato tubers [Dai et al. 2016].

Relative abundance of identified metabolites and proposed metabolomic pathway. The metabolomics pathway linked to the germination of Chinese yam bulbils was proposed, and a quantitative comparison of the normalised intensities of all detected compounds was performed (Fig. 5). The normalised intensities of all identified metabolites were quantitatively compared, and the metabolomics pathway associated with the germination of Chinese yam bulbils was proposed (Fig. 5). Carbohydrate metabolism, the TCA cycle, nitrogen metabolism, lipid metabolism, polyphenol metabolism, and phytosterol metabolism exhibited germination-associated dynamic changes. Bulbils serve as a means of vegetative reproduction for plants and contain large amounts of starch, lipids and proteins that make them analogous to starch-containing seeds such as mung bean [Chen et al. 2019] and brown rice [Kim et al. 2020]. Okagami [1986] found that the dormancy and germination characteristics of bulbils and seeds were similar. At the same time, the germination of Chinese yam bulbils may differ from seeds due

to dissimilar anatomical structures and perhaps environmental cue perception [Walck and Cofer 2010]. Similar to starch-containing seeds, bulbils break down stored macromolecules, including starch, lipids, and proteins, into monosaccharides, fatty acids, and amino acids by many enzymes to produce the energy needed for successful germination under certain environmental growth conditions. In addition, endogenous phenolic compounds are associated with germination in Chinese yam bulbils.

Carbohydrate metabolism is one of the critical metabolic routes that trigger and control germination and sprouting processes. Starch, sucrose, glucose, and raffinose metabolism took part in the germination and sprouting processes. These sugar molecules act as energy sources, signal transduction factors, and in phytohormone and stress responses during germination [Rolland et al. 2001]. The amounts of sucrose increased first and then decreased with the germination period. The levels of glucose slightly decreased until 3 days of germination, and after that, a significant increase in glucose levels was observed. The decrease in the relative content of glucose was caused by the consumption and conversion of sugar and the subsequent increase in the content was caused by the further hydrolysis of starch. Raffinose decreased with an increase in the germination period. Compared to the ungerminated bulbils (0 days), raffinose decreased by 9.8-fold in 15 days of germinated bulbils. These results were in accordance with the results of previous studies on mung bean seeds [Wu et al. 2020] and potato tubers [Dai et al. 2016]. Lactic acid, a product of anaerobic metabolism in seeds with hard seed coats [Sherwin and Simon 1969], is also present in the bulbils, probably because the bulbils also have a thicker cortex where hypoxia is expected. The best metabolic changes in lactic acid occurred after imbibition (1–15 days). These metabolites are involved in glycolysis and anaerobic respiration, and glycolysis may become the primary energy source for plant germination.

Malic acid and citric acid are essential intermediary products in the TCA cycle, and significantly larger relative concentrations in bulbils indicated higher TCA rates. The amount of malic acid increased constantly during the germination phase in the TCA cycle, and its levels on day 15 were 2.29 times larger than those in ungerminated bulbils (day 0), whereas citric

Table 1. Identification of metabolites contributing to the separation among sample groups on the OPLS-DA score plots of the dataset analysed by using UPLC-Q-TOF-MS in negative ion mode

	Identity	RT[a] (min)	Neutral mass (Da)	Observed m/z	Formula	Adducts	Error (ppm)	MS/MS fragmentation	VIP[b]	p-value[c]
1	Sucrose	0.83	342.11621	341.1085	C12H22O11	–H	–1.1	242.0914, 179.0654, 146.0539	4.11678	5.98×10^{-34}
2	Raffinose	0.83	504.16903	503.1625	C18H32O16	–H	1.6	496.1638, 488.1986, 341.1086, 179.0539	1.00653	2.90×10^{-32}
3	Aspartic acid	0.85	133.03751	132.0299	C4H7NO4	–H	–2.5	128.959	1.55806	1.10×10^{-37}
4	Glutamic acid	0.85	147.05316	146.0497	C5H9NO4	–H	2.6	113.0234	0.97307	5.13×10^{-08}
5	Glucose	0.86	180.06339	179.0556	C6H12O6	–H	–2.6	161.0452, 149.0453	1.02391	4.40×10^{-10}
6	Hypoxanthine	0.86	136.03851	195.0515	C5H4N4O	+CH3COO	–2.3	127.0572	0.93256	5.48×10^{-07}
7	3,4',5-Trihydroxy-3',7-dimethoxyflavone	0.87	332.0896	377.0873	C17H16O7	+HCOO	–2.7	296.8787, 179.0555	3.87946	2.90×10^{-32}
8	Allantoin	0.9	158.04399	157.0435	C4H6N4O3	–H	–2.2	113.0234, 101.0233	1.31685	1.59×10^{-12}
9	Malic acid	0.93	134.02152	133.0211	C4H6O5	–H	–2.9	119.0344, 101.0234	0.97195	2.96×10^{-07}
10	Lactic acid	0.94	90.03169	149.0452	C3H6O3	+CH3COO	–2.5	119.0356	3.11411	6.91×10^{-29}
11	Citric acid	1.03	192.027	191.0194	C6H8O7	–H	–1.9	111.0088	1.86373	6.18×10^{-27}
12	Tryptophan	2.6	204.08988	203.0866	C11H12N2O2	–H	1.9	159.1001, 146.9687	2.05169	2.70×10^{-24}
13	Kaempferol-3-O-rutinoside	3.65	594.15847	593.1509	C27H30O15	–H	–0.5	553.2574, 235.2960	1.24828	6.83×10^{-22}
14	Apiin	3.73	564.14791	563.1408	C26H28O14	–H	0.3	483.8685, 321.9283, 174.9644	1.2417	1.58×10^{-20}
15	p-Coumaric acid	4.02	164.04734	209.045	C9H8O3	+HCOO	–2.5	165.0632, 146.9712, 121.0355	1.04358	1.78×10^{-20}
16	Quercetin-3'-O-glucoside	4.24	464.09548	463.0877	C21H20O12	–H	–1	397.8072, 343.1015, 197.8210, 174.9671	0.81907	1.00×10^{-17}
17	3,3',5-Trimethoxybibenzyl	5.15	272.14124	331.1549	C17H20O3	+CH3COO	–0.5	221.8513, 197.8210, 146.9712	1.13001	1.21×10^{-16}
18	Protodioscin	5.84	1048.54542	1047.5377	C51H84O22	–H	–0.4	841.7038, 763.3410, 741.9727, 587.1958	2.32121	2.77×10^{-15}
19	Desgalactotigonin	5.86	1034.52977	1093.5407	C50H82O22	+CH3COO	–2.6	1083.5878, 989.8842, 778.3815, 595.2435	0.99311	1.60×10^{-14}
20	2,5-Dihydroxy-3,4-dimethoxyphenanthrene	8.35	270.08921	269.0813	C16H14O4	–H	–2.3	254.0566	3.40995	6.49×10^{-14}
21	Batatasin I	9.78	284.10486	283.0967	C17H16O4	–H	–3.2	153.8761	0.85122	2.06×10^{-13}
22	Dioscin	11.42	868.48204	913.4797	C45H72O16	+HCOO	–0.6	853.4982, 653.3463, 593.1765, 473.3212	2.64815	1.23×10^{-12}
23	Linolenic acid	12.1	278.22458	277.2167	C18H30O2	–H	–2.2	146.9617	1.89287	7.32×10^{-12}
24	Linoleic acid	15.91	280.24023	279.2327	C18H32O2	–H	–0.8	146.9712, 116.9360	4.32708	1.06×10^{-9}
25	Palmitic acid	16.82	256.24023	255.2324	C16H32O2	–H	–2.4	116.9274	1.95154	2.27×10^{-9}
26	Oleic acid	16.99	282.25588	281.2478	C18H34O2	–H	–2.7	255.2320, 116.9274	1.22825	4.25×10^{-8}
27	β-Daucosterol	17.33	576.43899	621.4367	C35H60O6	+HCOO	–0.8	159.0833	2.95774	6.48×10^{-11}

[a] RT was retention time.

[b] Variable importance in the projection (VIP) values was determined by OPLS-DA.

[c] p-value were analysed by ANOVA with Duncan's test.
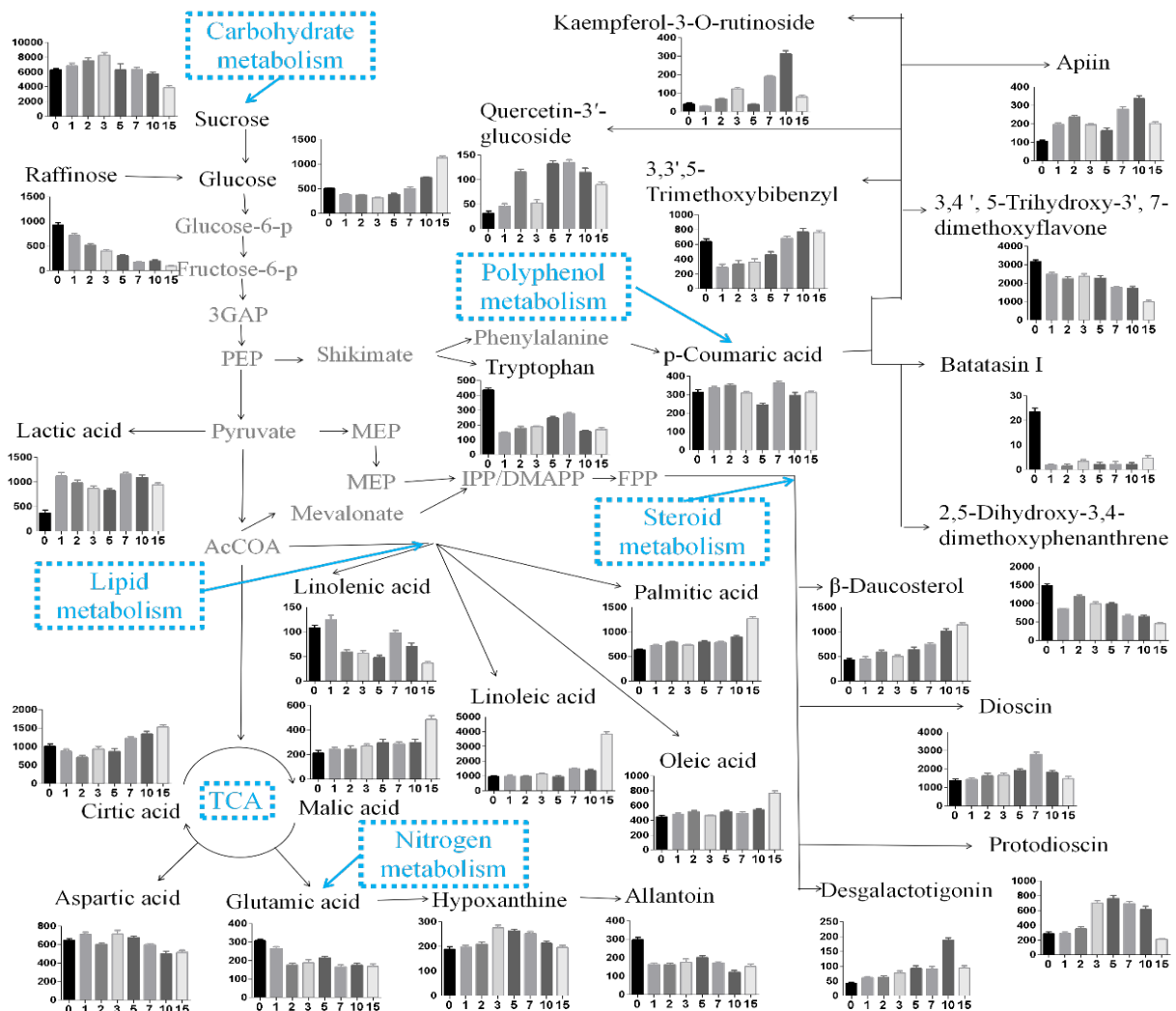
Fig 5. Metabolic map of the proposed association with energy production of Chinese yam bulbils during germination and the relative quantitative analysis of identified metabolites. The vertical axis of the bars represents the normalised chromatogram intensity, and the horizontal axis represents the germination period

acid declined for up to 3 days and then increased. Malic acid and citric acid also contributed indirectly to the increase in energy generation during germination.

Nitrogen metabolism is one of the primary metabolic pathways that triggers and governs germination processes. The development of plants depends on the associated physiological processes of synthesis, transformation, and degradation of proteins and amino acids [Osuna et al. 2015]. TCA cycle intermediates form glutamic acid, which is converted to glutamine and de novo synthesised to hypoxanthine and subsequently oxidised to allantoin. Allantoin is an essential bioactive compound in Chinese yam that improves diabetic symptoms [Ma et al. 2020], protects stomach tissues, and inhibits tumour growth [Lebot et al. 2019]. At the same time, allantoin has been the subject of investiga-

tion recently due to its triple function in nitrogen recycling, abiotic stress response and seed germination in plants [Ninomiya et al. 2008, Nourimand and Todd 2019, Wang et al. 2012]. Allantoin and glutamic acid levels were the highest at day 0 and then decreased. Our results suggest that the depletion of allantoin is a critical step of nitrogen metabolism in the germination of Chinese yam bulbils for nitrogen recycling and mobilisation. Moreover, crosstalk between nitrogen and carbohydrate metabolism helps to maintain the C/N balance, which in turn affects the germination and sprouting processes [Osuna et al. 2015]. The future research goal is to elucidate the molecular mechanisms of C and N-dependent signalling pathways in bulbil germination and plant development of Chinese yam through the implementation of "omics" science.

Lipids are also used as a compact energy source for Chinese yam bulbil germination. In the process of germination, free fatty acids are converted to acetyl–CoA by β–oxidation, and then acetyl–CoA units are converted to carbohydrates by the glyoxylate cycle in peroxisomes. In the early germination process, when the hydrolysis of starch is insufficient to supplement the decomposed sugars effectively, storage oil will be prematurely mobilised to convert lipids into sugars [Keawkim et al. 2021]. The contents of linolenic acid were the highest on day 2 and then significantly decreased, followed by a slight increase. The increase in linolenic acid at the beginning stage of the present study was similar to that in sacha inchi [Chandrasekaran and Liu 2015]. A variety of reasons can cause this phenomenon. On the one hand, they involve delays in the biosynthesis or activation of the lipase involved in this process, which is essential for fatty acid degradation. On the other hand, they involve a temporary inhibition of fatty acid breakdown under the action of excess soluble carbohydrates [Sun et al. 2019]. The amount of linoleic acid, palmitic acid and oleic acid increased slowly with germination time and significantly increased approximately 3, 1.8 and 1.3 times in 15-day germinated Chinese yam bulbils. The increase in linoleic acid, palmitic acid, and oleic acid concentrations shows that fatty acids may be biosynthesised during the later stages of germination, as observed for Chinese yam bulbils.

Plant phenolic metabolites, including hydroxycinnamic acids and flavonoids, are essential secondary metabolic substances during plant growth that play antimicrobial and antioxidant roles in the plant defence system [Islam et al. 2018]. In polyphenol metabolism, the amount of p-coumaric acid was higher in ungerminated and germinated Chinese yam bulbils and was not significantly changed by germination. Higher contents of p-coumaric acid in the non-germination and germination process of Chinese yam bulbils resulted in higher contents of phenolic compounds because *p*-coumaric acid is the precursor of many phenolics [Wang et al. 2016]. Batatasin I, 2,5-dihydroxy-3,4-dimethoxyphenanthrene and 3,4',5-trihydroxy-3',7-dimethoxyflavone dropped steadily for the entire germination period, and batatasin I was barely detected in the germination bulbil. Phenanthrene compounds, such as batatasin I, are essential factors in the dormancy of yam bulbils [Kim et al. 2010]. The contents of quercetin-3'-glucoside, kaempferol-3-O-rutinoside and api-in showed the same variation tendency and reached the highest amounts at the 10-day germinated bulbils, which are known as important bioactive compounds of flavonoids. PAL is an important and rate-limiting enzyme for the biosynthesis of flavonoids. The variation tendency of flavonoids was related to the activity of PAL during germination [Tomková-Drábková et al. 2016].

In addition to the metabolites associated with energy generation, some steroidal secondary metabolites, including β-daucosterol, dioscin, protodioscin, and desgalactotigonin, were identified. β-daucosterol was significantly increased with an increase in the germination period. Dioscin, protodioscin, and desgalactotigonin belong to the steroidal saponin class and are utilised as the main active ingredients of Chinese yam for coronary heart disease, tumour, inflammation, antioxidative, and tissue-protective properties [Cho et al. 2013, Li et al. 2021, Song et al. 2019]. The contents of dioscin, protodioscin, and desgalactotigonin increased in the middle stage of germination and then decreased. However, these three steroidal saponins did not change significantly before and after germination.

CONCLUSIONS

The changes in the metabolite profiles of Chinese yam bulbils during germination were analysed using UPLC-Q-TOF-MS, and differences in the samples

were visualised by PCA and OPLS-DA. Twenty-seven metabolites, including primary derivatives linked to energy production, such as organic acids, amino acids, sugars, and lipids, as well as secondary metabolites with different health advantages, such as phenolic and steroidal compounds, were found to be involved in the differences between the different groups on the PCA and OPLS-DA score plots. A metabolomics pathway was proposed based on the identified metabolites, and it was determined that carbohydrate metabolism, TCA cycle, nitrogen metabolism, lipid metabolism, polyphenol metabolism, and phytosterol metabolism were the main processes that changed during Chinese yam bulbil germination. The rapid decrease in the levels of allantoin, batatasin I, and raffinose could be utilised as an indicator of Chinese yam bulbil germination. However, the regulation and control of various metabolites throughout the entire germination process, as well as the impact of these metabolites on bulbil germination, are a series of highly complex problems. More research on joint sequential multi-omics analyses is required to better understand the complex physiological and biochemical mechanisms of bulbils at different stages of germination. The above results represent the first report on metabolite changes in germinating bulbils of Chinese yam. This study provides valuable information for the growth and development of Chinese yam plants.

SOURCE OF FUNDING

REFERENCES

Chandrasekaran, U., Liu, A. (2015). Stage-specific metabolization of triacylglycerols during seed germination of Sacha Inchi (*Plukenetia volubilis* L.). J. Sci. Food Agric. 95(8), 1764–1766. https://doi.org/10.1002/jsfa.6855

Chaniad, P., Tewtrakul, S., Sudsai, T., Langyanai, S., Kaewdana, K. (2020). Anti-inflammatory, wound healing and antioxidant potential of compounds from *Dioscorea bulbifera* L. bulbils. PLoS ONE, 15, e0243632. https://doi.org/10.1371/journal.pone.0243632

Chen, L., Wu, J.e., Li, Z., Liu, Q., Zhao, X., Yang, H. (2019). Metabolomic analysis of energy regulated germination and sprouting of organic mung bean (*Vigna radiata*) using NMR spectroscopy. Food Chem. 286, 87–97. https://doi.org/10.1016/j.foodchem.2019.01.183

Cho, J., Choi, H., Lee, J., Kim, M.-S., Sohn, H.-Y., Lee, D.G. (2013). The antifungal activity and membrane-disruptive action of dioscin extracted from *Dioscorea nipponica*. Biochim. Biophys. Acta, 1828(3), 1153–1158. https://doi.org/10.1016/j.bbamem.2012.12.010

Choi, K.-W., Um, S.H., Kwak, J.-H., Park, H.-J., Kim, K.-H., Moon, E.-Y., Kwon, S.-T., Pyo, S. (2012). Suppression of adhesion molecule expression by phenanthrene-containing extract of bulbils of Chinese yam in vascular smooth muscle cells through inhibition of MAPK, Akt and NF-κB. Food Chem. Toxicol. 50(8), 2792–2804. https://doi.org/10.1016/j.fct.2012.05.005

Dai, H., Fu, M., Yang, X., Chen, Q. (2016). Ethylene inhibited sprouting of potato tubers by influencing the carbohydrate metabolism pathway. J. Food Sci. Technol. 53(8), 3166–3174. https://doi.org/10.1007/s13197-016-2290-0

Dessalegn, O. (2016). Propagation methods of yam (*Dioscorea* species) with special attention to in vitro propagation. J. Appl. Biotechnol. 4(1), 13. https://doi.org/10.5296/jab.v4i1.9031

Drummond, C.P., Renner, T. (2022). Genomic insights into the evolution of plant chemical defense. Curr. Opin. Plant Biol. 68, 102254. https://doi.org/10.1016/j.pbi.2022.102254

Gu, E.-J., Kim, D.W., Jang, G.-J., Song, S.H., Lee, J.-I., Lee, S.B., Kim, B.-M., Cho, Y., Lee, H.-J., Kim, H.-J. (2017). Mass-based metabolomic analysis of soybean sprouts during germination. Food Chem. 217, 311–319. https://doi.org/10.1016/j.foodchem.2016.08.113

Gao, J., Ren, R., Wei, Y., Jin, J., Ahmad, S., Lu, C., Wu, J., Zheng, C., Yang, F., Zhu, G. (2020). Comparative metabolomic analysis reveals distinct flavonoid biosynthesis regulation for leaf color development of *Cymbidium sinense* 'Red Sun'. Int. J. Mol. Sci. 21(5), 1869. https://doi.org/10.3390/ijms21051869

Hill, C.B., Bacic, A., Roessner, U. (2014). LC-MS profiling to link metabolic and phenotypic diversity in plant mapping populations. Methods Mol. Biol. 1198, 29–41. https://doi.org/10.1007/978-1-4939-1258-2_3

Islam, M.T., Lee, B.-R., Das, P.R., La, V.H., Jung, H.-I., Kim, T.-H. (2018). Characterization of *p*-Coumaric acid-induced soluble and cell wall-bound phenolic metabolites

in relation to disease resistance to *Xanthomonas campestris* pv. *campestris* in Chinese cabbage. Plant Physiol. Biochem. 125, 172–177. https://doi.org/10.1016/j.plaphy.2018.02.012

Keawkim, K., Lorjaroenphon, Y., Vangnai, K., Jom, K.N. (2021). Metabolite–flavor profile, phenolic content, and antioxidant activity changes in Sacha Inchi (*Plukenetia volubilis* L.) seeds during germination. Foods 10(10), 2476. https://doi.org/10.3390/foods10102476

Kim, H., Kim, O.-W., Ahn, J.-H., Kim, B.-M., Oh, J., Kim, H.-J. (2020). Metabolomic analysis of germinated brown rice at different germination stages. Foods 9(8), 1130. https://doi.org/10.3390/foods9081130

Kim, S.K., Lee, S.C., Lee, B.H., Choi, H.J., Lee, I.J. (2010). Bulbil formation and yield responses of chinese yam to application of gibberellic acid, mepiquat chloride and trinexapac-ethyl. J. Agron. Crop Sci. 189(4), 255–260. https://doi.org/10.1046/j.1439-037X.2003.00039.x

Lebot, V., Faloye, B., Okon, E., Gueye, B. (2019). Simultaneous quantification of allantoin and steroidal saponins in yam (*Dioscorea* spp.) powders. J. Appl. Res. Med. Arom. Plants 13, 100200. https://doi.org/10.1016/j.jarmap.2019.02.001

Li, X., Liu, S., Qu, L., Chen, Y., Yuan, C., Qin, A., Liang, J., Huang, Q., Jiang, M., Zou, W. (2021). Dioscin and diosgenin: Insights into their potential protective effects in cardiac diseases. J. Ethnopharmacol. 274, 114018. https://doi.org/10.1016/j.jep.2021.114018

Ma, J., Meng, X., Liu, Y., Yin, C., Zhang, T., Wang, P., Park, Y.-K., Jung, H.W. (2020). Effects of a rhizome aqueous extract of *Dioscorea* batatas and its bioactive compound, allantoin in high fat diet and streptozotocin-induced diabetic mice and the regulation of liver, pancreas and skeletal muscle dysfunction. J. Ethnopharmacol. 259, 112926. https://doi.org/10.1016/j.jep.2020.112926

Mizuki, I., Ishida, K., Tani, N., Tsumura, Y. (2010). Fine-scale spatial structure of genets and sexes in the dioecious plant *Dioscorea japonica*, which disperses by both bulbils and seeds. Evol. Ecol. 24, 1399–1415. https://doi.org/10.1007/s10682-010-9396-z

Murty, Y.S., Purnima. (1983). Morphology, anatomy and development of bulbil in some dioscoreas. Proc. Plant Sci. 92, 443–449. https://doi.org/10.1007/BF03053017

Narula, A., Kumar, S., Bansal, K.C., Srivastava, P.S. (2003). *In vitro* micropropagation, differentiation of aerial bulbils and tubers and diosgenin content in *Dioscorea bulbifera*. Planta Med. 69(8), 778–779. https://doi.org/10.1055/s-2003-42781

Ninomiya, A., Murata, Y., Tada, M., Shimoishi, Y. (2008). Change in allantoin and arginine contents in *Dioscorea opposita* 'Tsukuneimo' during the growth. J. Japan. Soc. Hort. Sci. 73(6), 546–551. https://doi.org/10.2503/jjshs.73.546

Nourimand, M., Todd, C.D. (2019). There is a direct link between allantoin concentration and cadmium tolerance in Arabidopsis. Plant Physiol. Biochem. 135, 441–449. https://doi.org/10.1016/j.plaphy.2018.11.016

Okagami, N. (1986). Dormancy in *Dioscorea*: different temperature adaptation of seeds, bulbils and subterranean organs in relation to north-south distribution. Bot. Mag. Tokyo 99, 15–27. https://doi.org/10.1007/BF02488619

Osuna, D., Prieto, P., Aguilar, M. (2015). Control of seed germination and plant development by carbon and nitrogen availability. Front. Plant Sci. 6, 1023. https://doi.org/10.3389/fpls.2015.01023

Padhan, B., Panda, D. (2020). Potential of neglected and underutilized yams (*Dioscorea* spp.) for improving nutritional security and health benefits. Front. Pharmacol. 11, 496. https://doi.org/10.3389/fphar.2020.00496

Qu, C., Zuo, Z., Cao, L., Huang, J., Liu, G. (2019). Comprehensive dissection of transcript and metabolite shifts during seed germination and post-germination stages in poplar. BMC Plant Biol. 19, 1–15. https://doi.org/10.1186/s12870-019-1862-3

Rolland, F., Moore, B., Sheen, J. (2001). Sugar sensing and signaling in plants. Plant Cell 14(S1), S185-S205. https://doi.org/10.1105/tpc.010455

Sherwin, T., Simon, E.W. (1969). The appearance of lactic acid in phaseolus seeds germinating under wet conditions. J. Exp. Bot., 776–785. https://doi.org/10.1093/jxb/20.4.776

Song, S., Chu, L., Liang, H., Chen, J., Liang, J., Huang, Z., Zhang, B., Chen, X. (2019). Protective effects of dioscin against doxorubicin-induced hepatotoxicity via regulation of Sirt1/FOXO1/NF-κb signal. Front. Pharmacol. 10, 1030. https://doi.org/10.3389/fphar.2019.01030

Sun, J., Jia, H., Wang, P., Zhou, T., Wu, Y., Liu, Z. (2019). Exogenous gibberellin weakens lipid breakdown by increasing soluble sugars levels in early germination of zanthoxylum seeds. Plant Sci. 280, 155–163. https://doi.org/10.1016/j.plantsci.2018.08.013

Tomková-Drábková, L., Psota, V., Sachambula, L., Leišová-Svobodová, L., Mikyška, A., Kučera, L. (2016). Changes in polyphenol compounds and barley laccase expression during the malting process. J. Sci. Food Agric. 96(2), 497–504. https://doi.org/10.1002/jsfa.7116

Walck, J.L., Cofer, M.S., Hidayati, S.N. (2010). Understanding the germination of bulbils from an ecological perspective: a case study on Chinese yam (*Dioscorea polystachya*). Ann. Bot. 106(6), 945–955. https://doi.org/10.1093/aob/mcq189

Wang, G., Wu, L., Zhang, H., Wu, W., Zhang, M., Li, X.F., Wu, H. (2016). Regulation of the phenylpropanoid pathway: a mechanism of selenium tolerance in peanut (*Arachis hypogaea* L.) Seedlings. J. Agric. Food

Chem. 64(18), 3626–3635. https://doi.org/10.1021/acs.jafc.6b01054

Wang, P., Kong, C.-H., Sun, B., Xu, X.-H. (2012). Distribution and function of allantoin (5-ureidohydantoin) in rice grains. J. Agric. Food Chem. 60(11), 2793. https://doi.org/10.1021/jf2051043

Wu, X., Wang, Y., Tang, H. (2020). Quantitative metabonomic analysis reveals the germination-associated dynamic and systemic biochemical changes for mung-bean (*Vigna radiata*) seeds. J. Proteome Res. 19(6), 2457–2470. https://doi.org/10.1021/acs.jproteome.0c00181

Wu, Z.G., Jiang, W., Tao, Z.-M., Pan, X.J., Yu, W.H., Huang, H.-L. (2019). Morphological and stage-specific transcriptome analyses reveal distinct regulatory programs underlying yam (*Dioscorea alata* L.) bulbil growth. J. Exp. Bot. 71(6), 1899–1914. https://doi.org/10.1093/jxb/erz552

Yu, Y.-G., Guo, X.-Y., Li, X.-Y., Dai, D.-D., Xu, X.-R., Ge, X.-J., Li, Y.-J., Yang, T.-G. (2021). Organ- and age-specific differences of *Dioscorea polystachya* compounds measured by UPLC-QTOF/MS. Chem. Biodiversity 18(2), e2000856. https://doi.org/10.1002/cbdv.202000856

Zhang, S.R. (2014). Dioscoreaceae. In: Ai T.M. (ed.). Medicinal flora of China. 11th Ed. Peking, Peking University Medical Press, 48.

Zhang, B., Guo, K., Lin, L.S., Wei, C.X. (2018). Comparison of structural and functional properties of starches from the rhizome and bulbil of Chinese Yam (*Dioscorea opposita* Thunb.). Molecules 23(2), 427. https://doi.org/10.3390/molecules23020427